

Bayesian Graph Contrastive Learning

Arman Hasanzadeh¹, Mohammadreza Armandpour¹, Ehsan Hajiramezanali¹,
Mingyuan Zhou², Nick Duffield¹, Krishna Narayanan¹

¹Texas A&M University ²The University of Texas at Austin

¹{armanihm, armandpur1990, ehsanr, duffieldng, krn}@tamu.edu, ²mzhou@utexas.edu

Abstract

Contrastive learning has become a key component of self-supervised learning approaches for graph-structured data. However, despite their success, existing graph contrastive learning methods are incapable of uncertainty quantification for node representations or their downstream tasks, limiting their application in high-stakes domains. In this paper, we propose a novel Bayesian perspective of graph contrastive learning methods showing random augmentations leads to stochastic encoders. As a result, our proposed method represents each node by a distribution in the latent space in contrast to existing techniques which embed each node to a deterministic vector. By learning distributional representations, we provide uncertainty estimates in downstream graph analytics tasks and increase the expressive power of the predictive model. In addition, we propose a Bayesian framework to infer the probability of perturbations in each view of the contrastive model, eliminating the need for a computationally expensive search for hyperparameter tuning. We empirically show a considerable improvement in performance compared to existing state-of-the-art methods on several benchmark datasets.

1. Introduction

Recent self-supervised contrastive methods have shown great promise to produce high-quality node representations by learning to be invariant to different augmentations in graph domain. These methods generally learn the node embedding via maximizing the agreement between augmented views of the same node, while minimizing the agreement of views of different node [21, 25–27].

While these contrastive learning methods have achieved great empirical performance, to the best of our knowledge, all of them are limited to only learning a single deterministic embedding vector for each node. Therefore, they can neither capture the uncertainty of their learned embeddings nor quantify the uncertainty of predictions for downstream tasks. Uncertainty quantification is crucial in many im-

pactful real-life decision-making applications such as node classification in biological networks [7, 10, 16]. Another main challenges in graph contrastive learning methods is the proper choice of augmentation types and drop probabilities. While there has been works, mainly in vision, that learn parameters of augmentations during the training of a contrastive model, they have very restrictive assumptions. They either restrict each augmentation operation to be invertible [23] or only learn the probability of picking a specific type of augmentation and do not learn the parameters of the augmentations [25].

To address the first problem, we propose a novel Bayesian formulation of graph contrastive learning which offers a mathematically grounded framework to estimate uncertainty. More specifically, first we propose a generalized augmentation model where random augmentations are applied to each layer of encoders independently. Furthermore, we show that existing augmentation models are special cases of our generalized augmentation scheme. Next, we show that training a graph contrastive model with our generalized augmentation model is an approximation of a Variational Graph Auto-Encoder (VGAE) with a non-parametric likelihood and Bayesian graph neural networks as encoders. While, in our formulation, the conditional approximate posterior is delta distribution, the marginal approximate posterior is an implicit distribution. Having an implicit variational family as opposed to a parametric one, allows our model to better approximate the true posterior and consequently quantify uncertainty more accurately. Moreover, we derive a formulation for translating the uncertainty of representations to the downstream task. More specifically, we parametrize the predictive distribution of downstream model as countable mixture of parametric distributions (e.g. softmax for node classification or normal for node regression). Our flexible predictive model has more expressive power hence it is less prone to misspecification.

In addition, we develop a novel Bayesian method to learn the parameters of our generalized augmentation model. We show that our framework is an approximation of VGAE with a non-parametric likelihood. In this setting, the weight

parameters of graph neural network encoders are fixed while the parameters of our generalized augmentation are considered learnable. Furthermore, in our Bayesian model, we propose a hierarchical beta-Bernoulli construction for the augmentations. To the best of our knowledge, this is the first work in the contrastive learning literature that models augmentations as discrete random variable with learnable parameters.

Our overall proposed method, Bayesian Graph Contrastive Learning (BGCL), learns the parameters of contrastive model together with parameters of augmentations in a two stage process in each training epoch by optimizing two Evidence Lower Bounds (ELBOs). We empirically demonstrate that our BGCL outperforms existing methods on several benchmark dataset, both in terms of prediction accuracy and prediction uncertainty, i.e. Patch Accuracy Vs Patch Uncertainty (PAVPU) [16]. We emphasize that although our paper is focused on contrastive learning methods for graphs, we believe our work can motivate similar works in vision as such a model has not been developed or explored for vision datasets yet.

2. Preliminaries

2.1. Equivalency of InfoNCE and VAEs [1]

VAEs and self-supervised learning (SSL) methods are two class of models that aim to learn *good* representations of data. VAEs learn an encoder which maps data to latent representations, and learn a decoder which maps the latent representations back to the data. The parameters of encoder and decoder are learned by optimizing the evidence lower bound (ELBO). Let's consider a VAE which takes two observations, \mathbf{x} and \mathbf{x}' , and infers two latent variables, \mathbf{h} and \mathbf{h}' . Moreover, assume that the inference model is factorized as $q(\mathbf{h}, \mathbf{h}' | \mathbf{x}, \mathbf{x}') = q(\mathbf{h} | \mathbf{x}) q(\mathbf{h}' | \mathbf{x}')$, while the generative models is factorized as $p(\mathbf{h}, \mathbf{h}', \mathbf{x}, \mathbf{x}') = p(\mathbf{x} | \mathbf{h}) p(\mathbf{x}' | \mathbf{h}') p(\mathbf{h}, \mathbf{h}')$. Then, the ELBO for this VAE is defined as follows:

$$\mathcal{L}_{\text{VAE}} = \mathbb{E}_{q(\mathbf{h}, \mathbf{h}' | \mathbf{x}, \mathbf{x}')} \left[\log \frac{p(\mathbf{x} | \mathbf{h}) p(\mathbf{x}' | \mathbf{h}') p(\mathbf{h}, \mathbf{h}')}{q(\mathbf{h} | \mathbf{x}) q(\mathbf{h}' | \mathbf{x}')} \right]. \quad (1)$$

On the other hand, SSL methods take two augmented views of the same input \mathbf{x} and \mathbf{x}' , encode them to form two latent representations \mathbf{h} and \mathbf{h}' , and maximize the mutual information between them without reconstructing the observations. Estimating the mutual information is intractable, hence SSL methods derive a lower bound for it using a classifier that distinguishes the positive sample from negative samples. This type of loss, which is known as In-

foNCE [17, 21], is defined as follows:

$$\begin{aligned} \mathcal{I}(\mathbf{h}; \mathbf{h}') &= \mathbb{E}_{q(\mathbf{h}, \mathbf{h}')} \left[\log \frac{q(\mathbf{h}' | \mathbf{h})}{q(\mathbf{h}')} \right] \geq \mathcal{I}_{\text{NCE}}(\mathbf{h}; \mathbf{h}'); \\ \mathcal{I}_{\text{NCE}} &= \mathbb{E}_{q(\mathbf{h}, \mathbf{h}')} \underbrace{\left[\log \frac{g(\mathbf{h}, \mathbf{h}')}{g(\mathbf{h}, \mathbf{h}') + \sum_{j=1}^N g(\mathbf{h}, \mathbf{h}_j')} \right]}_{-\mathcal{L}_{\text{CNT}}} \\ &\quad + \log N, \end{aligned} \quad (2)$$

where g is a similarity function such as cosine similarity, and N is the number of negative samples. Existing SSL methods learn deterministic latent representations, i.e. $q(\mathbf{h} | \mathbf{x}) = \delta(\mathbf{h} - f(\mathbf{x}))$ with f as encoder function. Hence, the expectation with respect to posterior distribution of latent representations in the definition of \mathcal{I}_{NCE} (or \mathcal{L}_{CNT}) are often ignored.

To show that the ELBO (equation 1) is equivalent to \mathcal{I}_{NCE} (equation 2) for some specific choices of prior, posterior, and likelihood, [1] defines a non-parametric likelihood as follows:

$$\begin{aligned} p(\mathbf{x} | \mathbf{h}) &= \frac{q(\mathbf{h} | \mathbf{x}) p_{\text{true}}(\mathbf{x})}{q(\mathbf{h})}; \\ q(\mathbf{h}) &= \int q(\mathbf{h} | \mathbf{x}) p_{\text{true}}(\mathbf{x}) d\mathbf{x}, \end{aligned} \quad (3)$$

where $p_{\text{true}}(\mathbf{x})$ is the true distribution of data. We note that the same equations could be written for \mathbf{h}' and \mathbf{x}' . By substituting $p(\mathbf{x} | \mathbf{h})$ and $p(\mathbf{x}' | \mathbf{h}')$ terms in ELBO, we can rewrite it as:

$$\begin{aligned} \mathcal{L}_{\text{SS-VAE}} &= \mathbb{E}_{q(\mathbf{h}, \mathbf{h}' | \mathbf{x}, \mathbf{x}')} \left[\log \frac{p_{\text{true}}(\mathbf{x}) p_{\text{true}}(\mathbf{x}') p(\mathbf{h}, \mathbf{h}')}{q(\mathbf{h} | \mathbf{x}) q(\mathbf{h}' | \mathbf{x}')} \right] \\ &= \mathbb{E}_{q(\mathbf{h}, \mathbf{h}' | \mathbf{x}, \mathbf{x}')} \left[\log \frac{p(\mathbf{h}, \mathbf{h}')}{q(\mathbf{h}) q(\mathbf{h}')} \right] \\ &\quad + \log p_{\text{true}}(\mathbf{x}) + \log p_{\text{true}}(\mathbf{x}'), \end{aligned} \quad (4)$$

where SS-VAE stands for self-supervised VAE. The last two terms in the above equation are independent of parameters, hence they don't affect the optimization and could be treated as constants. By choosing specific prior distributions $p(\mathbf{h}, \mathbf{h}')$, we can recover the SSL objectives. For example, $p(\mathbf{h}, \mathbf{h}') = q(\mathbf{h}, \mathbf{h}')$ leads to $\mathcal{I}(\mathbf{h}; \mathbf{h}')$, while choosing the following priors recovers the infinite limit of \mathcal{I}_{NCE} ($N \rightarrow \infty$):

$$p(\mathbf{h}) = q(\mathbf{h}), \quad p(\mathbf{h}' | \mathbf{h}) = \frac{1}{\mathcal{H}} g(\mathbf{h}, \mathbf{h}') q(\mathbf{h}'); \quad (5)$$

where $\mathcal{H} = \int g(\mathbf{h}, \mathbf{h}') q(\mathbf{h}') d\mathbf{h}' = \mathbb{E}_{q(\mathbf{h}')} [g(\mathbf{h}, \mathbf{h}')]$.

Essentially, this shows that a contrastive model with InfoNCE loss is a VAE with an implicit likelihood and without reconstruction. While the analysis in this section provides an interesting interpretation of contrastive models, it fails to provide the uncertainty of representation as contrastive models embed data to deterministic latent variables.

2.2. Graph contrastive learning

Inspired by the success of contrastive methods in vision, graph contrastive learning methods have been introduced to learn node embeddings by minimizing a contrastive loss between two *augmented views* of the same graph. *Random corruptions* are applied to the input graph to obtain augmented views. The corruptions are chosen from a set of corruption types which usually includes $\mathbb{T} = \{\text{NodeDrop}, \text{EdgeDrop}, \text{FeatureDrop}, \text{SubgraphSelection}\}$. Although several graph contrastive losses have been proposed [22, 24, 27], the main goals of these objective functions are: 1) enforcing the representations of the same node in the two views of the graph to be close to each other, and 2) pushing apart representations of every other node.

To achieve the first goal, the vast majority of the methods include a term that measures the similarity between the representations of the same nodes in the two views (e.g. cosine similarity). For the second goal, different approaches have been proposed. For example, GRACE [27] deployed negative samples, like SimCLR [2], while BGRL [22] uses different encoders for each view in the same way as BYOL [5]. Without loss of generality, we carry out our analysis based on GRACE. We note that the same analysis could be applied to other methods as well.

Given a graph $\mathcal{G} = (\mathbf{A}, \mathbf{X})$ with $\mathbf{A} \in \mathbb{R}^{N \times N}$ as adjacency matrix and $\mathbf{X} \in \mathbb{R}^{N \times F_0}$ as attributes matrix, GRACE generate two views of the graph $\tilde{\mathcal{G}}_o = (\tilde{\mathbf{A}}_o, \tilde{\mathbf{X}}_o)$ and $\tilde{\mathcal{G}}_t = (\tilde{\mathbf{A}}_t, \tilde{\mathbf{X}}_t)$ by sampling from a random corruption function. Subscripts o and t are used for indexing two views. Next, a graph neural networks (GNN) f , is deployed to map the augmented graphs to latent representations, \mathbf{H}_o and \mathbf{H}_t , independently. The parameters of encoder (i.e. f) are learned by minimizing the following loss function:

$$\mathcal{L}_{\text{GRACE}} = \underbrace{\frac{-1}{2N} \sum_{i=1}^N [\ell(\mathbf{H}_{o,[i,:]}, \mathbf{H}_{t,[i,:]}) + \ell(\mathbf{H}_{t,[i,:]}, \mathbf{H}_{o,[i,:]})]}_{\mathcal{L}_{\text{CNT}}} + \underbrace{\lambda \sum_{j=1}^L \|\mathbf{W}^{(j)}\|_2^2}_{\mathcal{L}_{\text{WD}}};$$

$$\begin{aligned} \ell(\mathbf{H}_{o,[i,:]}, \mathbf{H}_{t,[i,:]}) &= \log \frac{e^{g(\mathbf{H}_{o,[i,:]}, \mathbf{H}_{t,[i:]})/\tau}}{e^{g(\mathbf{H}_{o,[i,:]}, \mathbf{H}_{t,[i:]})/\tau} + B_1 + B_2}; \\ B_1 &= \sum_{k=1}^N \mathbb{1}_{[k \neq i]} e^{g(\mathbf{H}_{o,[i,:]}, \mathbf{H}_{t,[k,:]})/\tau}, \\ B_2 &= \sum_{k=1}^N \mathbb{1}_{[k \neq i]} e^{g(\mathbf{H}_{o,[i,:]}, \mathbf{H}_{o,[k,:]})/\tau}, \end{aligned} \tag{6}$$

where τ is a hyperparameter, λ is a ℓ^2 weight decay hyperparameter, g is a similarity function, L is the number of layers in encoder, and $\mathbf{W}^{(j)}$ represents the parameters of the encoder at j -th layer. It has been shown that \mathcal{L}_{CNT} in the above equation is a lower bound for InfoNCE objective [27].

3. Method

In this section, we introduce our novel Bayesian formulation of graph contrastive learning– Bayesian Graph Contrastive Learning (BGCL). Unlike current methods which are limited to learning deterministic vector representations, our proposed model learns an *implicit distribution* for each node allowing to capture the uncertainty of latent representations. Moreover, we provide a natural Bayesian approach to translate the uncertainty of representation to the downstream predictive models such as node classification and regression.

3.1. Bayesian graph contrastive learning

We are interested in developing a Bayesian interpretation of contrastive models which can be used to quantify uncertainty of representations. To that end, we will: 1) introduce a generalized augmentation model and show that how the stochasticity of augmentations can be perceived as randomness in the parameters of the encoders; 2) show that the graph contrastive loss (equation 6) is equivalent to the ELBO of a variational autoencoder with stochastic function as encoder and specific choices of prior, posterior, and likelihood.

3.1.1 Generalized augmentation model

We first define a generalized augmentation method that includes the existing augmentation types as special cases. We note that all of the augmentations in \mathbb{T} (section 2.2) are simply parametrized by a random binary mask matrix. For example, FeatureDrop can be formulated as $\tilde{\mathbf{X}} = \mathbf{X} \odot \tilde{\mathbf{Z}}$, where \odot is the Hadamard product, and $\tilde{\mathbf{Z}}$ is a sample drawn from a random Bernoulli matrix.

Unlike existing works where augmentations are only applied at the first layer (i.e. input data) of encoders, we extend the notion of augmentation and propose to multiply the

output of each layer of encoders by a random mask. These masks could be drawn from different types and/or have different probability distributions. This extension allows us to view augmentation as a stochastic regularization technique in GNNs. Indeed, conventional augmentation is a stochastic regularization that is only being applied to the first layer of encoder.

Furthermore, to increase flexibility of the model, we propose to multiply a different random mask with the adjacency matrix for every input-output feature pair [8]. More specifically, the $(l + 1)$ -th layer of graph neural network in an encoder with generalized augmentation is defined as follows:

$$\mathbf{U}_{[:,j]}^{(l+1)} = \sigma \left(\sum_{i=1}^{F_l} g_a \left(\mathbf{A} \odot \tilde{\mathbf{Z}}^{(l,i,j)} \right) \mathbf{U}_{[:,i]}^{(l)} \mathbf{W}_{[i,j]}^{(l)} \right);$$

for $j = 1, \dots, F_{l+1}$,

where $\mathbf{U}^{(l)} \in \mathbb{R}^{N \times F_l}$ is the matrix of features at layer l with $\mathbf{U}^{(0)} = \mathbf{X}$, F_l is the number of features at layer l , σ is the activation function, g_a is the adjacency matrix normalization operator [13], and the elements of $\tilde{\mathbf{Z}}^{(l,i,j)}$ are drawn from Bernoulli($\pi^{(l)}$). It can be easily shown that existing augmentations are special cases of our proposed method. For example, choosing $\tilde{\mathbf{Z}}^{(l,i,j)} = \mathbf{1}_{N \times N} \text{diag}(\tilde{\mathbf{Z}}_{[:,i]}^{(l)})$ and $\pi^{(0)} \neq 1$ while $\{\pi^{(l)} = 1\}_{l=1}^{L-1}$ leads to FeatureDrop.

Having defined our generalized augmentation model, we show that the randomness could be transferred from input to parameters. To that end, we rewrite and reorganize equation 7 to have a node-wise view of the layers. More specifically,

$$\begin{aligned} \mathbf{U}_{[v,j]}^{(l+1)} &= \sigma \left(c_v \sum_{i=1}^{F_l} \sum_{u \in \{\mathcal{N}(v), v\}} \mathbf{U}_{[u,i]}^{(l)} \left(\tilde{\mathbf{Z}}_{[v,u]}^{(l,i,j)} \mathbf{W}_{[i,j]}^{(l)} \right) \right), \\ &= \sigma \left(c_v \sum_{i=1}^{F_l} \sum_{u \in \{\mathcal{N}(v), v\}} \mathbf{U}_{[u,i]}^{(l)} \tilde{\mathbf{W}}_{[i,j]}^{(l,u,v)} \right), \end{aligned} \quad (7)$$

where c_v is a constant depending on the graph structure, $\mathcal{N}(v)$ is the first hop neighborhood of v , and $\tilde{\mathbf{W}}_{[i,j]}^{(l,u,v)} := \tilde{\mathbf{Z}}_{[v,u]}^{(l,i,j)} \mathbf{W}_{[i,j]}^{(l)}$. This can be interpreted as learning different random weights for each of the connections in a GNN layer. Therefore, we refer to $\tilde{\mathbf{W}}^{(l,u,v)} = [\tilde{\mathbf{W}}_{[i,j]}^{(l,u,v)}]$ as connection-specific weights.

3.1.2 Bayesian interpretation

To show that a GCL model with generalized augmentation is a VAE with stochastic function as encoder, we must show that the $\mathcal{L}_{\text{CNT}} + \mathcal{L}_{\text{WD}}$ in equation 6 is a valid ELBO for such

a VAE. In section 2.1, it has been shown that contrastive learning methods are VAEs with deterministic functions as encoder and deterministic latent variables (i.e. delta distribution as posterior), hence \mathcal{L}_{CNT} is a valid ELBO. However, as pointed out in section 2.1, this is merely an interpretation and does not provide the uncertainty of representations. In order to get the uncertainty of representations, we propose to view encoders with generalized augmentation as stochastic functions. More precisely, we can view our proposed model as a VAE whose encoders (i.e. mapping from data to parameters of posteriors) are Bayesian neural networks. In this setting, the parameters of encoders and conditional posteriors have parametric form, while the marginal posteriors (i.e. $q(\mathbf{H}_o | \mathcal{G})$ and $q(\mathbf{H}_t | \mathcal{G})$) are *implicit* distributions.

Consider a variational graph autoencoder (VGAE) with two latent variables \mathbf{H}_o and \mathbf{H}_t and two Bayesian graph neural networks as encoders. Having stochastic encoders adds another set of latent variables to model, i.e. parameters of encoders denoted by $\mathcal{W} = \mathcal{W}_o \cup \mathcal{W}_t$ where $\mathcal{W}_o = \{\mathcal{W}_o^{(l)}\}_{l=1}^L = \{\{\tilde{\mathbf{W}}_o^{(l,u,v)}\}_{(u,v) \in \mathcal{E}}\}_{l=1}^L$ and $\mathcal{W}_t = \{\mathcal{W}_t^{(l)}\}_{l=1}^L = \{\{\tilde{\mathbf{W}}_t^{(l,u,v)}\}_{(u,v) \in \mathcal{E}}\}_{l=1}^L$. Furthermore, assume that the generative model is factorized as $p(\mathcal{G}, \mathbf{H}_o, \mathbf{H}_t, \mathcal{W}_o, \mathcal{W}_t) = p(\mathcal{G} | \mathbf{H}_o, \mathbf{H}_t) p(\mathbf{H}_o, \mathbf{H}_t) p(\mathcal{W}_o) p(\mathcal{W}_t)$ while the approximate posterior is factorized as $q(\mathbf{H}_o, \mathbf{H}_t, \mathcal{W}_o, \mathcal{W}_t | \mathcal{G}) = q(\mathbf{H}_o | \mathcal{G}, \mathcal{W}_o) q(\mathbf{H}_t | \mathcal{G}, \mathcal{W}_t) q(\mathcal{W}_o) q(\mathcal{W}_t)$. We can write the ELBO for this VGAE as follows:

$$\begin{aligned} \log p(\mathcal{G}) &= \log \mathbb{E}_{q(\mathbf{H}_o, \mathbf{H}_t, \mathcal{W} | \mathcal{G})} \left[\frac{p(\mathcal{G}, \mathbf{H}_o, \mathbf{H}_t, \mathcal{W}_o, \mathcal{W}_t)}{q(\mathbf{H}_o, \mathbf{H}_t, \mathcal{W}_o, \mathcal{W}_t | \mathcal{G})} \right] \\ &\geq \mathbb{E}_{q(\mathbf{H}_o, \mathbf{H}_t | \mathcal{G}, \mathcal{W})} \log \left[\frac{p(\mathcal{G} | \mathbf{H}_o, \mathbf{H}_t) p(\mathbf{H}_o, \mathbf{H}_t)}{\mathbb{E}_{q(\mathcal{W})} [q(\mathbf{H}_o | \mathcal{G}, \mathcal{W}_o) q(\mathbf{H}_t | \mathcal{G}, \mathcal{W}_t)]} \right] \\ &\quad + \mathbb{E}_{q(\mathcal{W})} \left[\log \frac{p(\mathcal{W}_o) p(\mathcal{W}_t)}{q(\mathcal{W}_o) q(\mathcal{W}_t)} \right] \\ &= \mathbb{E}_{(\mathbf{H}_o, \mathbf{H}_t | \mathcal{G}, \mathcal{W})} \log \left[\frac{p(\mathcal{G} | \mathbf{H}_o, \mathbf{H}_t) p(\mathbf{H}_o, \mathbf{H}_t)}{q(\mathbf{H}_o | \mathcal{G}) q(\mathbf{H}_t | \mathcal{G})} \right] \\ &\quad - D_{\text{KL}}(q(\mathcal{W}_o) || p(\mathcal{W}_o)) - D_{\text{KL}}(q(\mathcal{W}_t) || p(\mathcal{W}_t)) \\ &= \mathcal{L}_{\text{VGAE}}. \end{aligned} \quad (8)$$

We used Jensen's inequality in the derivation of ELBO above. Substituting the following non-parametric likelihood:

$$\begin{aligned} p(\mathcal{G} | \mathbf{H}_o, \mathbf{H}_t) &= \frac{q(\mathbf{H}_o | \mathcal{G}) q(\mathbf{H}_t | \mathcal{G}) p_{\text{true}}(\mathcal{G})}{q(\mathbf{H}_o) q(\mathbf{H}_t)}; \\ q(\mathbf{H}_o) &= \mathbb{E}_{p_{\text{true}}(\mathcal{G})} q(\mathcal{W}_o) q(\mathbf{H}_o | \mathcal{G}, \mathcal{W}_o), \\ q(\mathbf{H}_t) &= \mathbb{E}_{p_{\text{true}}(\mathcal{G})} q(\mathcal{W}_t) q(\mathbf{H}_t | \mathcal{G}, \mathcal{W}_t), \end{aligned} \quad (9)$$

in the definition of $\mathcal{L}_{\text{VGAE}}$, we have:

$$\begin{aligned} \mathcal{L}_{\text{BGCL}}^w &= \mathbb{E}_{(\mathbf{H}_o, \mathbf{H}_t | \mathcal{G}, \mathcal{W})} \log \left[\frac{p(\mathbf{H}_o, \mathbf{H}_t)}{q(\mathbf{H}_o) q(\mathbf{H}_t)} \right] \\ &\quad - D_{\text{KL}}(q(\mathcal{W}_o) || p(\mathcal{W}_o)) \\ &\quad - D_{\text{KL}}(q(\mathcal{W}_t) || p(\mathcal{W}_t)) + \log p_{\text{true}}(\mathcal{G}). \end{aligned} \quad (10)$$

Note that $\log p_{\text{true}}(\mathcal{G})$ is independent of parameters and can be treated as constant. Next, we define the parameterization of latent representations. Using the following prior distributions:

$$\begin{aligned} p(\mathbf{H}_o) &= q(\mathbf{H}_o), \quad p(\mathbf{H}_t | \mathbf{H}_o) = \frac{1}{\mathcal{H}} g(\mathbf{H}_o, \mathbf{H}_t) q(\mathbf{H}_t); \\ \mathcal{H} &= \mathbb{E}_{q(\mathbf{H}_t)} [g(\mathbf{H}_o, \mathbf{H}_t)], \end{aligned} \quad (11)$$

it is straightforward to show that the first term in the definition of $\mathcal{L}_{\text{SS-VGAE}}$ (equation 10) is equal to infinite limit of \mathcal{L}_{NCE} or equivalently $-\mathcal{L}_{\text{CNT}}$ in equation 6.

Finally, we define the parameterization for prior and posterior of \mathcal{W}_o and \mathcal{W}_t such that $D_{\text{KL}}(q(\mathcal{W}_o) || p(\mathcal{W}_o)) + D_{\text{KL}}(q(\mathcal{W}_t) || p(\mathcal{W}_t))$ is proportional to \mathcal{L}_{WD} in equation 6. More specifically, we parametrize the posterior of weights as follows:

$$\begin{aligned} q(\mathcal{W}) &= q(\mathcal{W}_o) q(\mathcal{W}_t) = \prod_{l=1}^L \prod_{(u,v) \in \mathcal{E}} [q(\tilde{\mathbf{W}}_o^{(l,u,v)}) \\ &\quad q(\tilde{\mathbf{W}}_t^{(l,u,v)})]; \\ q(\tilde{\mathbf{W}}_o^{(l,u,v)}) &= \pi_o^{(l)} \delta(\tilde{\mathbf{W}}_o^{(l,u,v)} - \mathbf{0}) \\ &\quad + (1 - \pi_o^{(l)}) \delta(\tilde{\mathbf{W}}_o^{(l,u,v)} - \mathbf{M}^{(l)}), \end{aligned} \quad (12)$$

where $\delta(\cdot)$ is the Dirac delta function, and $\{\pi_o^{(l)}, \pi_t^{(l)}, \mathbf{M}^{(l)}\}_{l=1}^L$ are the parameters of the posterior. Note that we use the same form of parametrization for both views and for brevity we wrote the posterior for first view only. We share $\theta_w = \{\mathbf{M}^{(l)}\}_{l=1}^L$ between two views while having separate drop probabilities for each view. To be able to evaluate the KL term analytically, the discrete quantised Gaussian can be adopted as the prior distribution as in [3]. Then, we can derive the KL divergence between the prior and posterior as:

$$\begin{aligned} D_{\text{KL}}(q(\tilde{\mathbf{W}}_o^{(l,u,v)}) || p(\tilde{\mathbf{W}}_o^{(l,u,v)})) &\propto \frac{(1 - \pi_o^{(l)})}{2} \|\mathbf{M}^{(l)}\|^2 \\ &\quad - \mathcal{H}(\pi_o^{(l)}), \end{aligned} \quad (13)$$

where $\mathcal{H}(\cdot)$ is the Shannon entropy of Bernoulli random variable. When the augmentation probabilities are fixed,

$\mathcal{H}(\pi_t^{(l)})$ and $\mathcal{H}(\pi_o^{(l)})$ are constants, hence the KL divergence is only proportional to ℓ^2 norm of the weights. Hence, with appropriate choice of ℓ^2 regularization hyperparameter, it will be equal to \mathcal{L}_{WD} in equation 6. Our analysis showed that training a contrastive model with our generalized augmentation model is a Bayesian approximation of a VAE with stochastic encoders.

Our proposed BGCL offers a novel and interesting perspective of contrastive learning. More specifically, it could be interpreted that our BGCL has no augmentation and the embeddings are generated by feeding the original data to two different stochastic functions (i.e. moving stochasticity from data to function). Indeed, our unique construction of stochastic encoders allows the model to mimic data augmentation. Whether any other type of stochastic function, such as neural processes, works the same way or not is an interesting avenue for future works.

3.2. Learnable Bayesian graph contrastive learning

In last section, we assumed that the augmentation probabilities are fixed. Finding optimal parameters for augmentation distributions is subject to computationally expensive and time consuming search over a set of possible hyperparameters. Here, we propose a Bayesian approach with variational inference to learn the parameters of our generalized augmentation.

We impose independent hierarchical beta-Bernoulli priors over augmentations. Specifically, we assume

$$\begin{aligned} \mathcal{Z}_{o,[i,j]}^{(l,u,v)} | \pi_o^{(l)} &\sim \text{Bernoulli}(\pi_o^{(l)}); \\ \pi_o^{(l)} &\sim \text{Beta}(c/L, c(L-1)/L), \end{aligned} \quad (14)$$

where c is a hyperparameter. Furthermore, we parametrize the posterior using Kumaraswamy-Bernoulli hierarchical distribution [14] as follows:

$$\begin{aligned} q(\mathcal{Z}_{o,[i,j]}^{(l,u,v)} | \pi_o^{(l)}) &= \text{Bernoulli}(\pi_o^{(l)}); \\ q(\pi_o^{(l)}) &= a_o^{(l)} b_o^{(l)} (\pi_o^{(l)})^{a_o^{(l)}-1} (1 - (\pi_o^{(l)})^{a_o^{(l)}})^{b_o^{(l)}-1}, \end{aligned} \quad (15)$$

where $a_o^{(l)}$ and $b_o^{(l)}$ are variational parameters. Note that we use the same form of parameterization for prior and posterior of both views and for brevity we wrote the prior and posterior for the first view only. We denote the parameters of our augmentation model by $\theta_a = \theta_{a,o} \cup \theta_{a,t} = \{a_o^{(l)}, b_o^{(l)}\}_{l=1}^L \cup \{a_t^{(l)}, b_t^{(l)}\}_{l=1}^L$. Furthermore, we represent the set of latent augmentation masks by $\mathcal{Z} = \mathcal{Z}_o \cup \mathcal{Z}_t = \{\{\mathbf{Z}_o^{(l,u,v)}\}_{(u,v) \in \mathcal{E}}\}_{l=1}^L \cup \{\{\mathbf{Z}_t^{(l,u,v)}\}_{(u,v) \in \mathcal{E}}\}_{l=1}^L$, and the set of augmentation drop rates by $\mathbf{\Pi} = \mathbf{\Pi}_t \cup \mathbf{\Pi}_o = \{\pi_t^{(l)}\}_{l=1}^L \cup \{\pi_o^{(l)}\}_{l=1}^L$.

The main goal here is learning ‘‘good’’ augmentations which should be reflected in the likelihood function. However, before defining the likelihood, we have to define what

makes “good” augmentations. [23] argues that a good set of views are those that share the minimal information necessary to perform well at the downstream task. Note that this is equivalent to *maximizing* contrastive loss. Following the same principle, we define a likelihood that places more mass on views with lower mutual information. Let’s consider the same VGAE that was introduced in the last section. While there we assumed that weights are random variable with fixed augmentation drop rates, here we assume that $\theta_w = \{\mathbf{M}^{(l)}\}_{l=1}^L$ are fixed and θ_a are variational parameters. Following the same analysis as last section, we can write the ELBO for this self-supervised VGAE as follows:

$$\begin{aligned} \mathcal{L}_{\text{BGCL}}^a &= \mathbb{E}_{(\mathbf{H}_o, \mathbf{H}_t | \mathcal{G}, \mathcal{Z}, \boldsymbol{\Pi})} \log \left[\frac{p(\mathbf{H}_o, \mathbf{H}_t)}{q(\mathbf{H}_o) q(\mathbf{H}_t)} \right] \\ &\quad - D_{\text{KL}}(q(\mathcal{Z}_o, \boldsymbol{\Pi}_o) || p(\mathcal{Z}_o, \boldsymbol{\Pi}_o)) \\ &\quad - D_{\text{KL}}(q(\mathcal{Z}_t, \boldsymbol{\Pi}_t) || p(\mathcal{Z}_t, \boldsymbol{\Pi}_t)) \\ &\quad + \log p_{\text{true}}(\mathcal{G}). \end{aligned} \quad (16)$$

Now, let’s assume that the prior and posterior of latent representation are defined as follows:

$$\begin{aligned} p(\mathbf{H}_o) &= q(\mathbf{H}_o), \quad p(\mathbf{H}_t | \mathbf{H}_o) = \frac{1}{\mathcal{H}} g(\mathbf{H}_o, \mathbf{H}_t)^{-1} q(\mathbf{H}_t); \\ \mathcal{H} &= \mathbb{E}_{q(\mathbf{H}_t)} [g(\mathbf{H}_o, \mathbf{H}_t)^{-1}]. \end{aligned} \quad (17)$$

By substituting the above priors in equation 16, and using Jensen’s inequality, we can see that the first term in $\mathcal{L}_{\text{BGCL}}^a$ is lower bounded by the infinite limit of $-\mathcal{I}_{\text{NCE}}$ or equivalently \mathcal{L}_{CNT} . Furthermore, we can expand the KL terms in $\mathcal{L}_{\text{BGCL}}^a$ as follows:

$$\begin{aligned} &D_{\text{KL}}(q(\mathcal{Z}_o, \boldsymbol{\Pi}_o) || p(\mathcal{Z}_o, \boldsymbol{\Pi}_o)) \\ &= \sum_{l=1}^{L_o} \sum_{(u,v) \in \mathcal{E}} D_{\text{KL}}(q(\mathbf{Z}_o^{(l,u,v)}, \pi_o^{(l)}) || p(\mathbf{Z}_o^{(l,u,v)}, \pi_o^{(l)})) \\ &= \sum_{l=1}^{L_o} \sum_{(u,v) \in \mathcal{E}} D_{\text{KL}}(q(\mathbf{Z}_o^{(l,u,v)} | \pi_o^{(l)}) || p(\mathbf{Z}_o^{(l,u,v)} | \pi_o^{(l)})) \\ &\quad + D_{\text{KL}}(q(\pi_o^{(l)}) || p(\pi_o^{(l)})). \end{aligned}$$

Since the conditional posterior and prior of latent augmentation masks have the same distribution, i.e. Bernoulli, the KL divergence between them is zero. Hence, the KL term only depends on the KL divergence between posterior and prior of augmentation drop rates, which can be written as follows:

$$\begin{aligned} &D_{\text{KL}}(q(\pi_o^{(l)}) || p(\pi_o^{(l)})) = \\ &\quad \sum_{l=1}^L \left[\frac{a_o^{(l)} - c_o/L}{a_o^{(l)}} \left(-\gamma - \Psi(b_o^{(l)}) - \frac{1}{b_o^{(l)}} \right) \right. \\ &\quad \left. + \log \frac{a_o^{(l)} b_o^{(l)}}{c_o/L} - \frac{b_o^{(l)} - 1}{b_o^{(l)}} \right], \end{aligned}$$

where c_o is a hyperparameter, γ is the Euler-Mascheroni constant and $\Psi(\cdot)$ is the digamma function. Note that for brevity we wrote the last two equations for the first view only as the second view has the same form.

Due to the discrete nature of the random masks \mathcal{Z} , we cannot directly apply reparameterization trick to calculate the gradient of the KL term. Hence, we propose to use continuous approximation, i.e. concrete relaxation [3, 9], of \mathcal{Z} instead of discrete variables. This allows us to efficiently sample from a simple distribution. Given a drop probability π and a sample from uniform distribution $u \sim \text{Unif}[0, 1]$, a sample from concrete distribution can be calculated as follows:

$$\text{sigmoid} \left(\frac{1}{t} \left(\log \left(\frac{\pi}{1-\pi} \right) + \log \left(\frac{u}{1-u} \right) \right) \right),$$

where t is temperature parameter.

Having defined the augmentation learning method, we describe the overall learning procedure. We have two objective functions: 1) the objective function for contrastive model (equation 6 or equivalently equation 10) which is used for learning the parameters of encoders θ_w , and 2) the ELBO for our Bayesian augmentation learning method (equation 16) which is used for learning the parameters of augmentation θ_a . Combining these objective functions, we derive the overall objective of our model as:

$$\begin{aligned} &\min_{\theta_w} \mathcal{L}_{\text{CNT}} + \mathcal{L}_{\text{WD}} \\ &\max_{\theta_a} \mathcal{L}_{\text{CNT}} + D_{\text{KL}}(q(\mathcal{Z}, \boldsymbol{\Pi}) || p(\mathcal{Z}, \boldsymbol{\Pi})) \end{aligned} \quad (18)$$

In each training epoch, we first optimize the parameters of encoders by minimizing the contrastive loss. Next we optimize the parameters of augmentations by maximizing the ELBO for our Bayesian augmentation learning method.

We emphasize that to the best of our knowledge, this is the first method that models augmentations as discrete random variables which offers modeling more diverse types of augmentation. Moreover, our novel Bayesian framework with robust variational inference enables efficient estimation of parameters of augmentation.

3.3. Downstream predictive model

In section 3.1.2, by performing variational inference for the Bayesian contrastive learning model parameters, we learn the variational distribution over model’s weights. Therefore, by sampling from model’s weights variational density and passing the graph to the model, we will have approximate posterior samples for node embedding. In fact, these samples of the node embeddings are an implicit variational approximation $Q(\mathbf{H})$ of the true posterior density. Let $\mathbf{y} = \{y_v\}_{v \in \mathcal{V}}$ be the observed node classes in the graph. Non-Bayesian algorithms model the following probability

distribution:

$$\mathbf{y} \sim p_{\text{cat}}(\mathbf{y}; \text{Softmax}(\mathbf{H} \mathbf{W}_c)); \quad \mathbf{H} = f(\mathbf{X}, \mathbf{A})$$

where \mathbf{H} is the matrix learned node representations, \mathbf{W}_c is the parameters of the multinomial logistic regression and p_{cat} is referring to PMF of categorical distribution. However, in our case, f is a stochastic process rather than deterministic function, and we have samples of \mathbf{H} from the implicit distribution $Q(\mathbf{H})$. Therefore, our model become:

$$\mathbf{y} \sim p_{\text{cat}}(\mathbf{y}; \text{Softmax}(\mathbf{H} \mathbf{W}_c)); \quad \mathbf{H} \sim Q(\mathbf{H})$$

which allow us to calculate the likelihood of \mathbf{y} using:

$$p(\mathbf{y}) = \int p_{\text{cat}}(\mathbf{y}; \text{Softmax}(\mathbf{H} \mathbf{W}_c)) Q(\mathbf{H}) d\mathbf{H}. \quad (19)$$

Similar formulation can also be obtained for the regression task by replacing the categorical distribution with normal density with a fixed variance and not using softmax function for the mean.

In the non-Bayesian contrastive learning setup, a common practice for learning the parameters \mathbf{W}_c is via maximum log-likelihood. We also take the same approach, however, we do not have a closed-form likelihood. Therefore, we circumvent this problem by using the Monte Carlo estimate of the likelihood (equation 19) as:

$$\frac{1}{K} \sum_{i=1}^K p_{\text{cat}}(\mathbf{y}; \text{Softmax}(\mathbf{H}^{(i)} \mathbf{W}_c)); \quad \mathbf{H}^{(i)} \stackrel{iid}{\sim} Q(\mathbf{H}) \quad (20)$$

and learn the model parameter \mathbf{W}_c by maximizing the logarithm of the above term and batch-optimization. Our model is more flexible with higher expressive power compared to the existing methods. More specifically, based on equation 20, the proposed framework learns a mixture of categorical (normal) distributions rather than a single one for the classification (regression) task. Therefore, it is less prone to misspecification, providing more reliable predictions.

4. Experiments

4.1. Datasets

We use three standard graph datasets to benchmark the performance of BGCL as well as baselines. Cora [20], Citeseer [20], and Amazon-Photos [15]. Cora and Citeseer are citation datasets where each node represents a document and the edges indicate the citation relations. Each node is provided with a multi-dimensional binary attribute vector, where each dimension of the attribute vector indicates the presence of a word from a dictionary in the publication. We follow the same pre-processing steps as [27] and randomly split the nodes into train (10%) and test (90%) sets. Amazon-Photo is from the Amazon co-purchase graph

Table 1. Graph dataset statistics.

Dataset	Nodes	Edges	Features	Classes
Cora	2,708	5,429	1,433	7
Citeseer	3,327	4,732	3,703	6
Amazon-Photo	7,650	119,081	745	8

where nodes represent products and edges are between pairs of products frequently purchased together. Products are classified into eight classes, and node attributes are a bag-of-words representation of a product’s reviews. We follow the same pre-processing steps as [22] and randomly split the nodes into train/validation/test sets (10/10/80%), respectively. Table 1 provides the detailed statistics of the graph datasets used in our experiments.

4.2. Baselines and experimental setups

Since GRACE achieves the state-of-the-art results in graph contrastive learning, we use it as the base contrastive model in our BGCL. More specifically, we use our learnable Bayesian generalized augmentation approach on top of GRACE. For a fair comparison with baselines, we use the same set of hyperparameters as GRACE except for the augmentation drop rates which are learned in the training process. The prior distribution for all of the drop rates, $\pi^{(l)}$ s, is Beta(1, 1). The temperature in concrete distribution is 0.3. The linear classifiers are trained for 50 different random splits and random initializations. We implemented our model in PyTorch [18]. All of our simulations are conducted on a single NVIDIA Tesla P100 GPU node. We compare our BGCL with several baselines and state-of-the-art methods in terms of node classification accuracy. More specifically, we compare our BGCL with two contrastive methods (**GRACE** [27] and **DGI** [21]), two auto-encoders (**VGAE** and **GAE** [12]), two conventional node embedding methods (**node2vec** [6] and **DeepWalk** [19]), and **supervised GCN** [13]. We use the same setup for baselines as described in [27]. Since there are no contrastive models with uncertainty quantification capabilities, we compare our BGCL with two supervised models, Bayesian GCN with **Graph DropConnect (GDC)** [8] and Bayesian GCN with **DropOut (DO)** [8]. We use the same setup as [8] to quantify uncertainty for Cora dataset. Supplementary materials include more details on experimental setups.

4.3. Numerical results

4.3.1 Classification accuracy

The node classification accuracy of our BGCL and baselines are summarized in Table 2. We can see that BGCL outperforms all of the unsupervised, self-supervised, and supervised baselines in all of the datasets. We make a few obser-

Table 2. Performance of our BGCL and baselines on node classification in terms of accuracy (in %). The highest performance of unsupervised models is highlighted in boldface.

Method	Cora	Citeseer	Amazon-Photo
Raw features	64.8	64.6	78.53
node2vec	74.8	52.3	89.72
DeepWalk	75.7	50.5	89.44
DeepWalk + features	73.1	47.6	90.05
GAE	76.9	60.6	91.68
VGAE	78.9	61.2	92.24
DGI	82.6±0.4	68.8±0.7	91.61±0.22
GRACE	83.3±0.4	72.1±0.5	92.15±0.24
BGCL	83.77±0.28	72.71±0.25	92.51±0.15
Supervised GCN	82.8	72.0	92.42

variations: 1) Comparing BGCL and supervised GCN shows that our model infers latent representation that are highly generalizable by extracting useful information; 2) Our generalized augmentation method can model more complex perturbations between views compared to conventional augmentations; 3) Our learnable generalized augmentation scheme successfully learns optimal drop rates in an unsupervised setting. Note that although contrastive models are self-supervised, optimal augmentation types/probabilities are chosen via extensive grid search based on the performance of downstream task.

4.3.2 Uncertainty quantification

Ideally, if a model is confident about its prediction, the prediction should be accurate (i.e. high $p(\text{accurate} | \text{certain})$). Also, if a model is inaccurate on an output, it should be uncertain about the same output (i.e. high $p(\text{uncertain} | \text{inaccurate})$). These two probabilities can be combined into one to form metric for quality of uncertainty called Patch Accuracy Vs Patch Uncertainty (PAVPU) [16]. More specifically, $\text{PAVPU} = (n_{ac} + n_{iu}) / (n_{ac} + n_{au} + n_{ic} + n_{iu})$, where n_{ac} is the number of accurate and certain predictions, n_{au} is the number of accurate and uncertain predictions, n_{ic} is the number of inaccurate and certain predictions, and n_{iu} is the number of inaccurate and uncertain predictions. A model with higher PAVPU quantifies uncertainty better. While measuring accuracy is straightforward, different metric can be used to measure certainty. We use predictive entropy (as defined in [16]).

Figure 1 shows performance of BGCL and two supervised Bayesian GCN models in uncertainty quantification on Cora dataset. It is outperforming competing methods by a significant margin on most of the certainty thresholds. This is indeed very impressive considering that BGCL is a self-supervised model. This empirically proves that our novel Bayesian formulation of graph contrastive learning

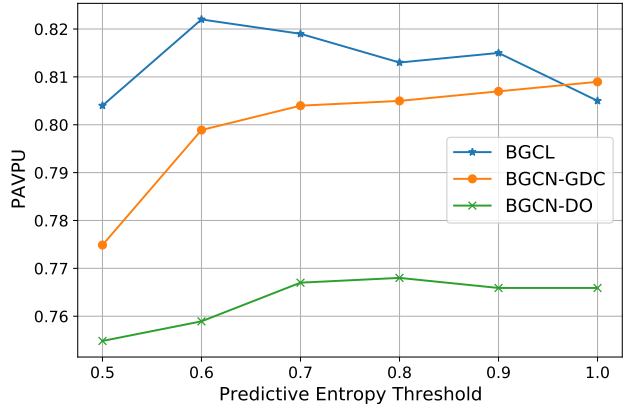


Figure 1. Comparison of uncertainty estimates in PAVPU by a 128-dimensional 4-layer Bayesian GCN with GDC, a 128-dimensional 4-layer Bayesian GCN with DropOut, and BGCL on Cora. The training and test sets are the same for all methods.

allows us to accurately capture uncertainty of latent representations.

5. Limitations

The main limitation of our proposed method is computational and space complexity of sampling generalized augmentations. As described in section 3.1.1, in our generalized augmentation model, we need to draw $F_i \times F_{i+1} \times E$ with E as number of edges. To alleviate this issue, we use a single sample for a block of features as oppose to drawing a new sample for every input-output feature pairs. This reduces the number of samples to $B \times E$ with B being number of blocks. In our experiments we use 8 blocks of feature, which decreases the training time substantially. Each training epoch of our BGCL on Cora dataset takes 0.884 seconds compared to GRACE which takes 0.016 seconds.

6. Conclusions

In this paper, we proposed Bayesian Graph Contrastive Learning (BGCL). First, we introduced a generalized augmentation method by applying random augmentation to each layer of encoders, independently. Next, we show that a graph contrastive learning model with the proposed augmentation method, can be perceived as a VGAE with Bayesian neural networks as encoder. As a result, our BGCL represents each node by a distribution in the latent space instead of deterministic node embeddings. Hence, BGCL provides predictive uncertainty in downstream graph analytics tasks. Furthermore, we developed a Bayesian framework to infer the augmentation drop rates in each view of the contrastive model, eliminating the need for a computationally expensive search for hyperparameter tuning.

References

- [1] Laurence Aitchison. Infonce is a variational autoencoder. *arXiv preprint arXiv:2107.02495*, 2021. [2](#)
- [2] Ting Chen, Simon Kornblith, Mohammad Norouzi, and Geoffrey Hinton. A simple framework for contrastive learning of visual representations. In *International conference on machine learning*, pages 1597–1607. PMLR, 2020. [3](#)
- [3] Yarin Gal, Jiri Hron, and Alex Kendall. Concrete dropout. In *Advances in neural information processing systems*, pages 3581–3590, 2017. [5, 6](#)
- [4] Xavier Glorot and Yoshua Bengio. Understanding the difficulty of training deep feedforward neural networks. In Yee Whye Teh and Mike Titterton, editors, *Proceedings of the Thirteenth International Conference on Artificial Intelligence and Statistics*, volume 9 of *Proceedings of Machine Learning Research*, pages 249–256, Chia Laguna Resort, Sardinia, Italy, 13–15 May 2010. PMLR. [11](#)
- [5] Jean-Bastien Grill, Florian Strub, Florent Altché, Corentin Tallec, Pierre Richemond, Elena Buchatskaya, Carl Doersch, Bernardo Avila Pires, Zhaohan Guo, Mohammad Gheshlaghi Azar, Bilal Piot, koray kavukcuoglu, Remi Munos, and Michal Valko. Bootstrap your own latent - a new approach to self-supervised learning. In H. Larochelle, M. Ranzato, R. Hadsell, M. F. Balcan, and H. Lin, editors, *Advances in Neural Information Processing Systems*, volume 33, pages 21271–21284. Curran Associates, Inc., 2020. [3](#)
- [6] Aditya Grover and Jure Leskovec. node2vec: Scalable feature learning for networks. In *Proceedings of the 22nd ACM SIGKDD international conference on Knowledge discovery and data mining*, pages 855–864, 2016. [7](#)
- [7] Ehsan Hajiramezani, Arman Hasanzadeh, Nick Duffield, Krishna R Narayanan, Mingyuan Zhou, and Xiaoning Qian. Variational graph recurrent neural networks. In *Advances in Neural Information Processing Systems*, 2019. [1](#)
- [8] Arman Hasanzadeh, Ehsan Hajiramezani, Shahin Boluki, Mingyuan Zhou, Nick Duffield, Krishna Narayanan, and Xiaoning Qian. Bayesian graph neural networks with adaptive connection sampling. In *Proceedings of the 37th International Conference on Machine Learning*, volume 119, pages 4094–4104. PMLR, 13–18 Jul 2020. [4, 7](#)
- [9] Eric Jang, Shixiang Gu, and Ben Poole. Categorical reparameterization with gumbel-softmax. *arXiv preprint arXiv:1611.01144*, 2016. [6](#)
- [10] Alex Kendall and Yarin Gal. What uncertainties do we need in bayesian deep learning for computer vision? *arXiv preprint arXiv:1703.04977*, 2017. [1](#)
- [11] Diederik P Kingma and Jimmy Ba. Adam: A method for stochastic optimization. *arXiv preprint arXiv:1412.6980*, 2014. [11](#)
- [12] Thomas N Kipf and Max Welling. Variational graph autoencoders. *arXiv preprint arXiv:1611.07308*, 2016. [7](#)
- [13] Thomas N Kipf and Max Welling. Semi-supervised classification with graph convolutional networks. In *International Conference on Learning Representations*, 2017. [4, 7, 10](#)
- [14] Ponnambalam Kumaraswamy. A generalized probability density function for double-bounded random processes. *Journal of Hydrology*, 46(1-2):79–88, 1980. [5](#)
- [15] Julian McAuley, Christopher Targett, Qinfeng Shi, and Anton Van Den Hengel. Image-based recommendations on styles and substitutes. In *Proceedings of the 38th international ACM SIGIR conference on research and development in information retrieval*, pages 43–52, 2015. [7](#)
- [16] Jishnu Mukhoti and Yarin Gal. Evaluating bayesian deep learning methods for semantic segmentation. *arXiv preprint arXiv:1811.12709*, 2018. [1, 2, 8, 11](#)
- [17] Aaron van den Oord, Yazhe Li, and Oriol Vinyals. Representation learning with contrastive predictive coding. *arXiv preprint arXiv:1807.03748*, 2018. [2](#)
- [18] Adam Paszke, Sam Gross, Francisco Massa, Adam Lerer, James Bradbury, Gregory Chanan, Trevor Killeen, Zeming Lin, Natalia Gimelshein, Luca Antiga, Alban Desmaison, Andreas Kopf, Edward Yang, Zachary DeVito, Martin Raison, Alykhan Tejani, Sasank Chilamkurthy, Benoit Steiner, Lu Fang, Junjie Bai, and Soumith Chintala. Pytorch: An imperative style, high-performance deep learning library. In H. Wallach, H. Larochelle, A. Beygelzimer, F. d'Alché-Buc, E. Fox, and R. Garnett, editors, *Advances in Neural Information Processing Systems 32*, pages 8024–8035. Curran Associates, Inc., 2019. [7](#)
- [19] Bryan Perozzi, Rami Al-Rfou, and Steven Skiena. Deepwalk: Online learning of social representations. In *Proceedings of the 20th ACM SIGKDD international conference on Knowledge discovery and data mining*, pages 701–710. ACM, 2014. [7](#)
- [20] Prithviraj Sen, Galileo Namata, Mustafa Bilgic, Lise Getoor, Brian Galligher, and Tina Eliassi-Rad. Collective classification in network data. *AI magazine*, 29(3):93, 2008. [7](#)
- [21] Fan-Yun Sun, Jordan Hoffmann, Vikas Verma, and Jian Tang. InfoGraph: Unsupervised and semi-supervised graph-level representation learning via mutual information maximization. *arXiv preprint arXiv:1908.01000*, 2019. [1, 2, 7](#)
- [22] Shantanu Thakoor, Corentin Tallec, Mohammad Gheshlaghi Azar, Remi Munos, Petar Veličković, and Michal Valko. Bootstrapped representation learning on graphs. In *ICLR 2021 Workshop on Geometrical and Topological Representation Learning*, 2021. [3, 7](#)
- [23] Yonglong Tian, Chen Sun, Ben Poole, Dilip Krishnan, Cordelia Schmid, and Phillip Isola. What makes for good views for contrastive learning? *arXiv preprint arXiv:2005.10243*, 2020. [1, 6](#)
- [24] Petar Veličković, William Fedus, William L. Hamilton, Pietro Liò, Yoshua Bengio, and R Devon Hjelm. Deep graph infomax. In *International Conference on Learning Representations*, 2019. [3](#)
- [25] Yuning You, Tianlong Chen, Yang Shen, and Zhangyang Wang. Graph contrastive learning automated. *International Conference on Machine Learning, ICML*, 2021. [1](#)
- [26] Yuning You, Tianlong Chen, Yongduo Sui, Ting Chen, Zhangyang Wang, and Yang Shen. Graph contrastive learning with augmentations. *Advances in Neural Information Processing Systems*, 33, 2020. [1](#)
- [27] Yanqiao Zhu, Yichen Xu, Feng Yu, Qiang Liu, Shu Wu, and Liang Wang. Deep graph contrastive representation learning. *arXiv preprint arXiv:2006.04131*, 2020. [1, 3, 7, 11](#)

In this supplement, we first provide additional results on representation uncertainty. Further implementation details are also presented.

A. Representation uncertainty

While previously we showed the performance of model in quantifying uncertainty of predictions in down stream task, here we provide results showing how uncertainty of representations increases the interpretability of our model. More specifically, we show that adding noise to input data (which can be seen as out of distribution samples), will increase the uncertainty of representation.

To that end, we first train our BGCL model on Cora, Citeseer and Amazon-photo datasets. Then, we randomly select a few nodes (10 for Cora and Citeseer, and 100 for Amazon-photo), and replace their attributes with normally distributed noise ($\mathcal{N}(0, 1)$ for Cora and Citeseer, and $\mathcal{N}(0, 1)$ and $\mathcal{N}(0, 10)$ for Amazon-photo). We train our BGCL model on these noisy datasets as well. We examine the difference between the Average Standard Deviation (ASTD) of latent representations of the randomly selected nodes in the two cases. We do the same examination for k -hop neighbors (for $k = 1, \dots, 5$) of the randomly selected nodes as well. Note that given s Monte-Carlo samples from d -dimensional latent representation of a node (denoted by a $d \times s$ matrix), the ASTD is calculated by first calculating the standard deviation along the second dimension and then averaging over the first dimension.

Figures 2 and 3 show the box plot of the difference between ASTDs of latent representations of randomly selected nodes (as well as their k -hop neighbors) in noisy and noise-free versions of Cora and Citeseer. Note that 0-hop neighbors refers to the randomly selected nodes themselves. We can see that the noisy nodes have the highest increase in ASTD. The reason for higher ASTD in noisy case is that information mismatch between the attribute of noisy

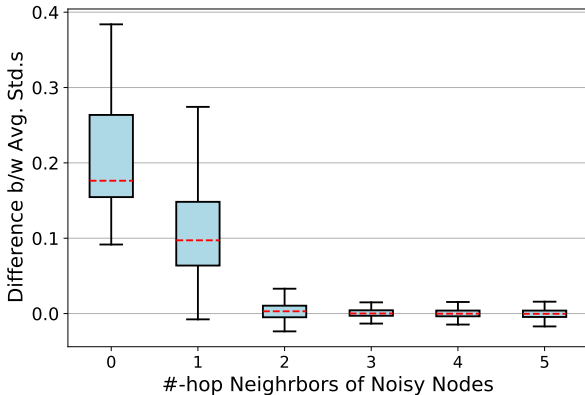


Figure 2. Cora

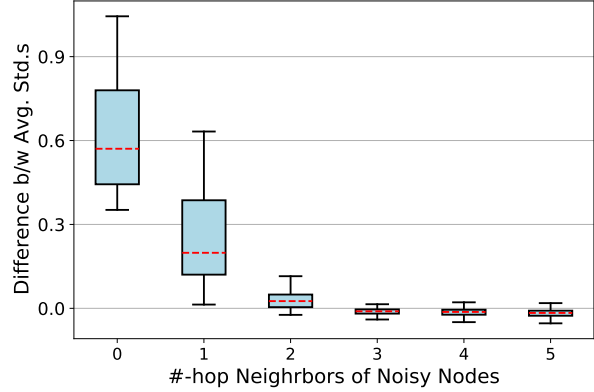


Figure 3. Citeseer

nodes and their neighbors. As we go farther away from the noisy nodes, the difference gets closer to zero. Noting that GCNs [13] are graph filters, this observation is consistent with evolution of a diffusion process over graph. Figure 4 shows the results for Amazon-photo dataset. We can see that adding $\mathcal{N}(0, 1)$ does not effect the ASTD significantly. This can be explained by higher average degree of Amazon-photo (31.13) compared to Cora (3.90) and Citeseer (2.77). Having more neighbors allows the model to filter out noise and learn embeddings with higher confidence. By increasing the standard deviation of noise to 10, we can see the effect of noise. As expected, we see the same behavior as Cora and Citeseer.

B. Further implementation details

Table 3 shows the hyperparameters used in our experiments for each dataset. LR_w in Table 3 refers to learning rate for the first step of optimization while LR_a denotes the learning rate for the second step of optimization. Note that, for a fair comparison, hidden dimension, latent dimension, activation function, and τ are the same as experiments in

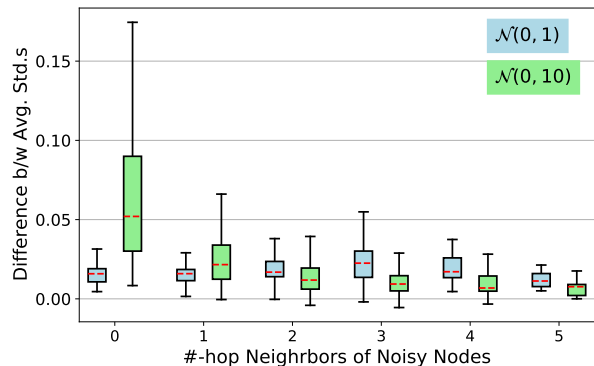


Figure 4. Amazon-Photo

Table 3. Hypeparameter specifications.

Dataset	LR_w	LR_a	ℓ_2	# of blocks	Epochs	Hidden dim	Latent dim	Activation	τ
Cora	0.0005	0.001	5×10^{-9}	8	250	256	128	ReLU	0.4
Citeseer	0.001	0.0005	5×10^{-9}	8	250	512	256	PReLU	0.9
Amazon-Photo	0.001	0.0005	5×10^{-9}	2	250	512	256	PReLU	0.7

GRACE [27]. For simplicity, we assumed that the augmentation in all layers of a view have the same drop rate. All models are initialized with Xavier initialization [4], and trained using Adam optimizer [11]. For down-stream classification task, we have implemented our linear classifier in PyTorch. For all of the datasets, we train the classifier for 150 epochs using Adam optimizer with the learning rate of 0.1.

To calculate PAVPU (section 4.3.2), we first draw 500 random augmentations from the trained BGCL model leading to 500 embeddings for each node. Next, we train a classifier (as described in section 3.3) using 10 samples. Then, we deploy the trained classifier to predict the nodes' labels using the remaining 49 sets of 10 samples. Having 49 prediction for each node, we follow the same procedure as in [16] to calculate PAVPU.